EXPERIMENTAL POOL BOILING INVESTIGATIONS OF VERTICAL COALESCENCE FOR FC-72 ON SILICON FROM AN ISOLATED ARTIFICIAL CAVITY

C. Hutter[1], A. Sanna[2], K. Sefiane[1,*], D.B.R. Kenning[2], T.G. Karayiannis[2], R.A. Nelson[3], H. Lin[1], G. Cummins[1], A.J. Walton[1]
[1]University of Edinburgh, Edinburgh, United Kingdom
[2]Brunel University, London, United Kingdom
[3]Los Alamos National Laboratory, Los Alamos, USA

ABSTRACT. In this study bubble growth from an isolated artificial cavity micro-fabricated on a horizontal 380 μm thick silicon wafer was investigated. The horizontally oriented boiling surface was heated by a thin resistance heater integrated on the rear of the silicon test section. The temperature was measured using an integrated micro-sensor situated on the boiling surface with the artificial cavity located in its geometrical centre. A resistive track was used as the sensor, which when calibrated, exhibited a near-linear behaviour with increasing temperature. To conduct pool boiling experiments the test section was immersed in degassed fluorinert FC-72. Bubble nucleation, growth and detachment at different pressures were observed using high-speed imaging. Coalescence was observed at the boundary between the isolated bubble and interference regimes. The occurrence of vertical coalescence was found to be more frequent, with increasing wall superheat and decreasing pressure.

The equivalent sphere volumes of two bubbles before and after coalescence were evaluated from area measurements. It was observed that the second nucleated bubble is always smaller than its predecessor. The vapour generation appears not to stop during coalescence as the volume of the merged bubble was typically 5-18% larger than the sum of the bubble volumes just before coalescence.

Keywords: *Nucleate Pool Boiling, Vertical Coalescence, Artificial Cavity*

INTRODUCTION

Nucleate boiling heat transfer remains as a potential cooling solution for high-performance micro-processors. Despite the intensive research over the last decades, a comprehensive understanding of many aspects and mechanisms is still not available. One of these aspects is vertical coalescence. In general, coalescence is a hydrodynamic direct interaction between bubbles, as they collide and hence merge into one larger bubble.

Zuber [1] separated nucleate boiling into two regions, the regime of isolated bubbles and the region of interference. The isolated bubble regime in nucleate pool boiling has been discussed in many publications [2]. In this regime, bubbles are produced intermittently and do not interfere with each other. When the wall superheat increases, the waiting time between the nucleation of a new bubble and the departure of the previous bubble, grown from the same site, becomes shorter. If a certain critical temperature is reached, succeeding bubbles merge to form a mushroom-like bubble. This merger can also involve pairs consisting of a large bubble followed by a small one departing from
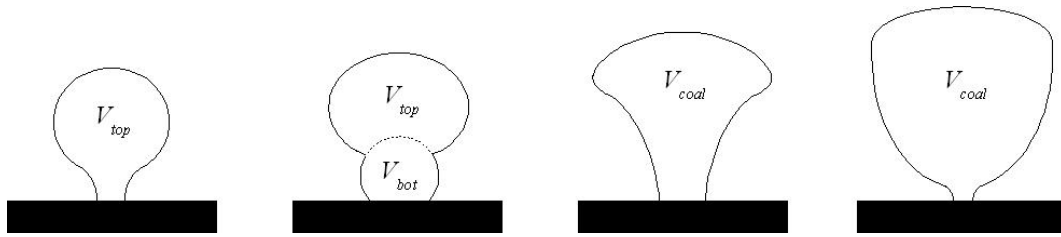
Figure 1. Vertical coalescence of two succeeding bubbles from an artificial nucleation site. The bubble with the volume V_{top} merges with the bubble with the volume V_{bot} to form a bubble of the volume V_{coal}.

the same nucleation site. This is known as the region of interference; bubbles interfere with each other and form continuous vapour columns and patches.

Buyevich and Webbon [3] investigated the limit of the isolated bubble regime. They identified four contributing mechanisms that lead to this limit, a) the upward flow of the rising bubble which obstructs the downward flow of liquid required to compensate for the vapour removal from the wall, b) lateral coalescence of bubbles from several nucleation sites to form large bubbles and extended vapour patches on the surface, c) longitudinal coalescence close to the wall, which results in the departure of dissimilar sized bubble pairs as mentioned before, d) longitudinal coalescence in the bulk, which leads to the formation of vapour columns. Buyevich and Webbon identified the last case as the most important effect for the termination of the isolated bubble region, as it can lead to the boiling crisis and trigger the critical heat flux.

Zhang and Shoji [4] classified 3 types of coalescence, i.e. vertical, horizontal and declining coalescence. Vertical coalescence occurs when during its growth phase a bubble touches the previously departed bubble, which is then drawn into and pulled away from the hot surface as illustrated in Figure 1.

Horizontal coalescence happens between two or more adjacent growing bubbles, which merge to form one large bubble. The merger of a growing bubble with an already departed bubble from an adjacent nucleation site is called declining coalescence. Zhang and Shoji concluded that bubble coalescence near the heated wall promotes growing bubbles to depart from the nucleation site. However, because vertical coalescence can occur for single and adjacent multiple nucleation sites, only horizontal and declining coalescence were thoroughly analysed. Although vertical coalescence is mentioned in several publications, this type of bubble interaction is usually not given much attention in the boiling heat transfer literature.

The bubbles in this study are growing from one isolated artificial cavity acting as nucleation site, allowing control of the location of the active site. Artificial cavities are widely used in boiling heat transfer research and mainly manufactured using microfabrication. Vapour or gas trapped in a cavity acts as a nucleus for the growth of a bubble. Bankoff [5] formulated the first criterion for pre-existing nuclei. This paper focuses on vertical coalescence occurring during nucleate pool boiling in the region of interference from an isolated artificial cavity. Coalescence is a hydrodynamic direct interaction between bubbles, as they collide and hence merge into one larger bubble. This is only of interest when occurring close to the heated surface, because away from the surface the impact on the boiling heat transfer is small [6].

EXPERIMENTAL SETUP

The working fluid was fluorinert FC-72, which is widely used for boiling experiments due to its non-toxicity, non-flammability and its low boiling temperature ($T_{sat} = 57.15$ °C at $p = 1$ bar). Its good dielectric properties make it possible to immerse the bare electrical connections to the 380 μm thick
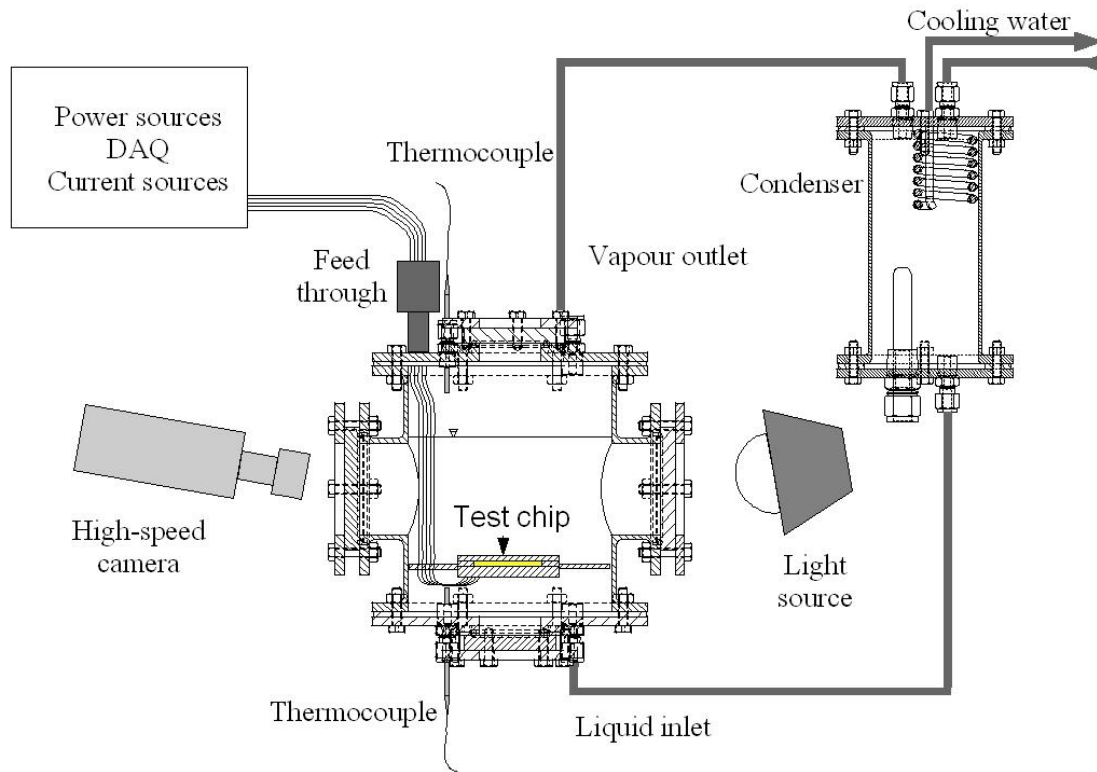
Figure 2. Experimental setup including the main parts boiling chamber
with test section, condenser, high-speed camera and backlight source.

silicon test section into the liquid. Electrical connections from the silicon chip are made through an air-tight feed-through in the wall of the stainless steel boiling chamber to provide the interconnect to the DAQ, the power supply for the integrated resistance heater and the constant current sources for the integrated micro-sensors. The chamber has four windows for optical access to the test section as shown in Figure 2. The wall temperature of the chamber is controlled by two silicone heater pads wrapped around the chamber. Four heater elements at the bottom of the chamber are used for degassing and bringing the liquid to the set temperature. Two thermocouples inside the chamber measure the temperature of the liquid and the vapour. If they indicate the same temperature, the saturation pressure has been reached and saturated boiling is taking place. The pressure in the chamber is measured by a calibrated pressure transducer with measurement error smaller than 0.2%. Boiling can be maintained at any pressure between 0.5 and 3 bar by adjusting the condenser cooling water flow with a valve and the temperature with a heating bath.

An isolated cylindrical artificial cavity with a mouth diameter of 10±0.5 μm and a depth of 80±5 μm was micro-fabricated on the top surface of the silicon test section. A Ti/Ni micro-sensor with a square shape covering an area of 0.84 mm x 0.84 mm was deposited around the artificial cavity. The silicon chip was held in place and, except for the actual boiling surface, insulated with a frame made of PEEK, which has similar thermal properties to PTFE. Spring probes were used, in order to ensure a good electrical contact between the integrated heater and sensor on the chip and the wires. The resistance of the sensor was calibrated using a standard thermometer and exhibits a near linear behaviour with temperature.

After the boiling liquid is thoroughly degassed and the set pressure reached, boiling from the artificial cavity is initiated with the resistance heater integrated on the rear of the silicon wafer. Bubble growth is observed with a high-speed camera and a backlight source positioned on the opposite side. The temperature readings from the micro-sensor are simultaneously acquired through a trigger. Synchronisation is necessary to correlate measurements to video recordings and will be

essential to link small changes in local wall temperatures to the bubble dynamics in future studies. In this paper the sensors are used to measure the time averaged wall surface temperature in the immediate vicinity of the nucleation site for the duration of recording. The limit of error is 0.5 K for all wall superheat measurements and the standard deviation is within the error. However, no error bars are indicated in the plots in order to improve legibility. The heat flux was measured with a voltage and current meter and has an error of ±1%.
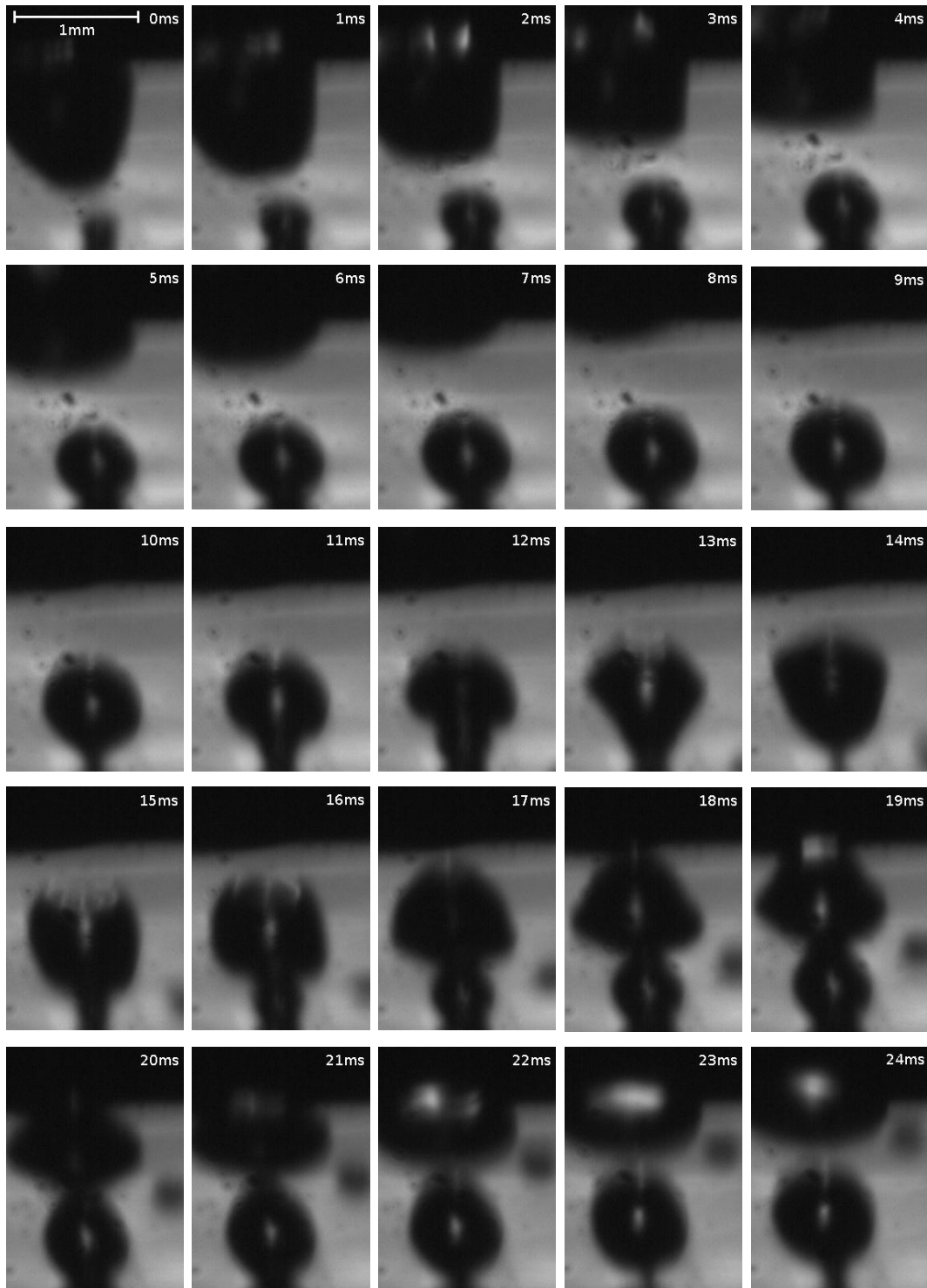
Fig. 3: Bubble growth sequence including vertical coalescence for a wall superheat of 7.9 K (applied heat flux 4.8 kW/m^2) at an absolute pressure of 0.5 bar. The first frame includes a scale.
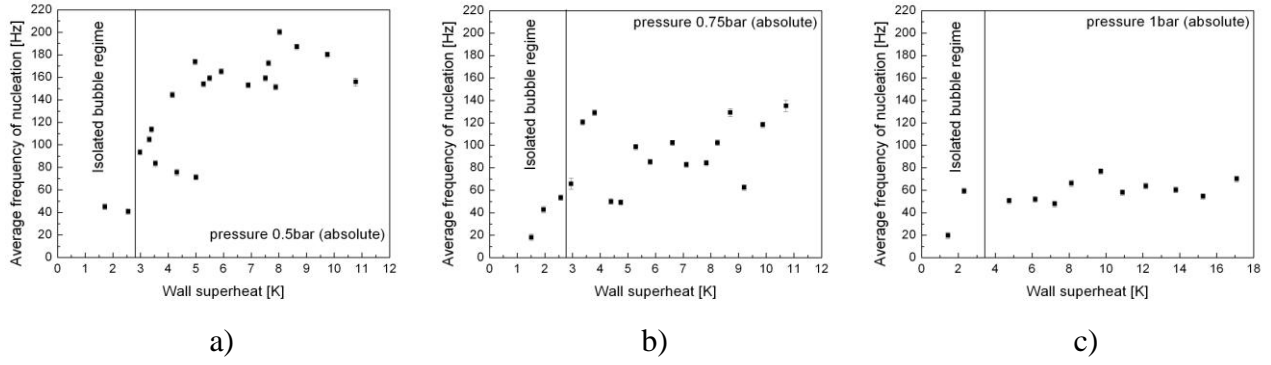
Figure 4. Average frequency of nucleation with increasing wall superheat
for a) 0.5 bar, b) 0.75 bar and c) 1 bar.

EXPERIMENTAL RESULTS AND DISCUSSION

The lowest possible wall superheat is limited by the internal temperature of the nucleus, which must equal the saturation temperature for the pressure of the vapour phase in order for the nucleus not to shrink. It is calculated from the Laplace equation:

$$p_g - p_l = \frac{2\sigma}{r_b} \tag{1}$$

where p_g is the vapour pressure, p_l the pressure of the liquid, σ the surface tension and r_b the nucleus curvature radius which equals the cavity mouth diameter r_c. For 0.5 bar, 0.75 bar and 1 bar the minimum temperature differences are 1.98 K, 1.29 K and 0.94 K.

The average frequency of nucleated bubbles and vertical coalescence from an isolated single cavity were measured using high-speed images for absolute pressures of 0.5 bar, 0.75 bar and 1 bar with increasing wall temperature superheat. Figure 3 presents a sequence of bubble growth at 0.5 bar absolute pressure and a wall superheat of 7.9 K (applied heat flux 4.8 kW/m^2) with camera set to 1000 fps. Bubble nucleation occurs at 0 ms and for the first 11 ms the bubble growth follows the common behaviour of a single bubble. At 11 ms a second bubble nucleates from the same artificial cavity and within 3 ms completely merges with the previously departed upper bubble. At 15 ms a third bubble nucleates, but does not coalesce with its predecessor during growth. The occasionally visible widening of the bubble base is due to reflection of the bubble on the silicon surface.

Figure 4 shows the average nucleation frequency with increasing wall superheat for the above three pressures. With increasing pressure the number of nucleations per second decreases. With increasing wall superheat this number of nucleations initially increases sharply and seems to level off, with this behaviour being more pronounced for the 0.5 bar pressure case. The results for 0.75 bar are rather scattered and for 1 bar the initial increase is less noticeable.

Figure 5 presents the average frequency of vertical coalescence for the same three pressures with increasing wall superheat. Lowering the pressure or increasing the wall superheat increases the occurrence of coalescence. The average frequency of bubble nucleation corresponds to an increase in the average frequency of vertical coalescence, as coalescence tends to reduce the bubble growth time. Bubbles are pulled away from the surface at much smaller size and this increases the number of nucleations for the same time period but increases the total growth time of the two bubbles only by a few milliseconds.

Figure 6 compares the average frequency of vertical coalescence with the number of nucleations (*VC/Nu*). At 0.5 bar approximately 50% of the bubbles coalesce for higher wall superheats. The
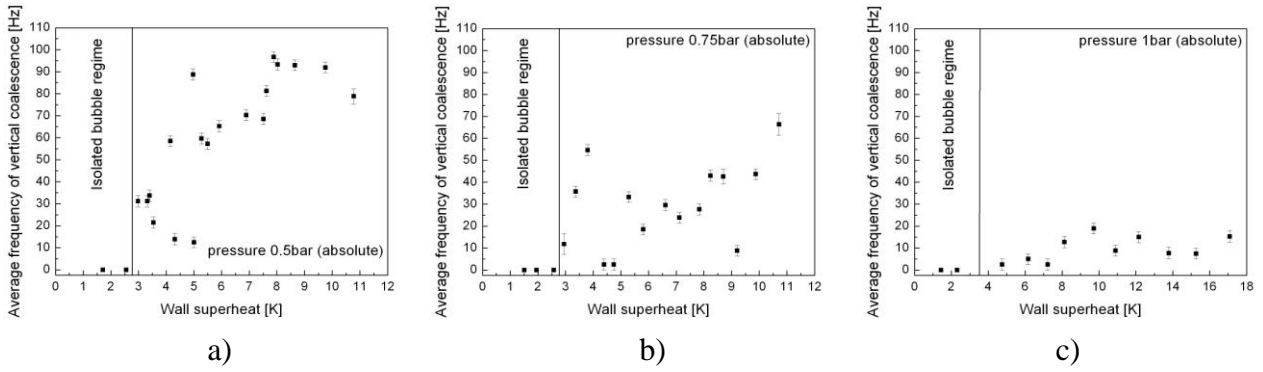
Figure 5. Average frequency of vertical coalescence with
increasing wall superheat for a) 0.5 bar, b) 0.75 bar and c) 1 bar.

ratio remains at this level even with increasing wall superheats. A possible explanation for this behaviour might be the fact that vertical coalescence most commonly appears only in pairs, i.e. only very rarely does a third bubble coalesce with already vertically coalesced bubbles. As the pressure increases, the ratio between vertical coalescence and nucleations decreases. For 1bar the maximum ratio is around 0.2 for high wall superheats. This means that around three bubbles depart as single bubbles before vertical coalescence occurs between the two that follow. Measurements for 0.75 bar tend to lie in between the results for the lower and higher pressure.

Following the above observations the volumes of ten bubble pairs immediately before and after coalescence are presented. The pressure was 0.5 bar with a wall superheat of 7.9 K (applied heat flux 4.8 kW/m^2). Bubble vapour volumes were estimated from high speed image sequences and Figure 7 presents an example sequence. The original images were processed with the software PCO Picture Viewer and a suitable threshold helped to identify the bubble area. The program then solved the equation:

$$V = \pi \int_0^y r_b(y)^2 dy \qquad (2)$$

where $r_b(y)$ is the bubble radius depending on the vertical position. The volume was scaled with a reference image loaded into the software. The measurement error was estimated to be ±0.005mm for the bubble radius. Due to the invisibility of the intersection between the top and bottom bubble the shape of the bottom bubble was assumed to be spherical. Since small single bubbles have a small Eötvös or Bond number, gravitational effects are negligible and the shape is near spherical.
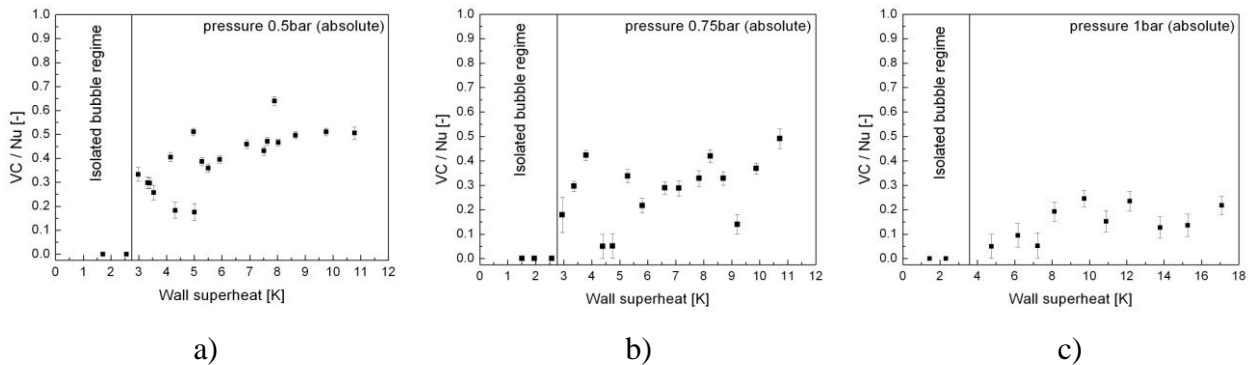
Figure 6. Ratio of the average frequency of vertical coalescence and
bubble nucleation with increasing wall superheat for a) 0.5bar, b) 0.75bar
and c) 1bar.

a)   b)   c)
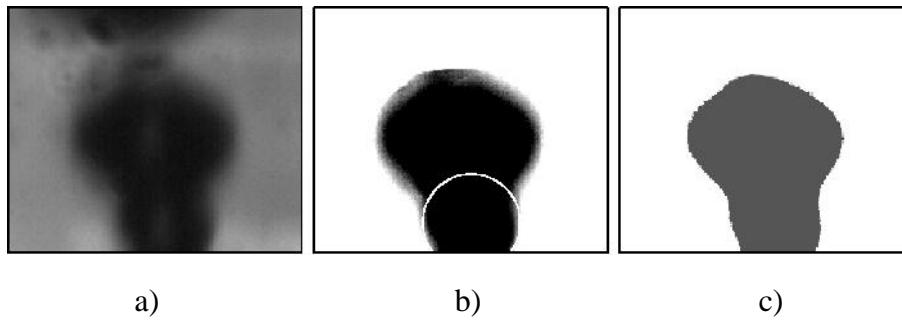
Figure 7. a) Original image during bubble growth with vertical coalescence. b) Processed picture with the assumed shape of the bottom bubble indicated. c) Area measured with PCO Picture Viewer software. From this area the volume of revolution is calculated.

Figure 8 a) shows the results with the systematic measurement error indicated. The newly nucleated bubble (bottom bubble) is always smaller than the previously departed one (top bubble) and the total volume immediately after coalescence is larger than the sum of volumes before the coalescence. Figure 8 b) shows the ratio between the volume of the bottom bubble V_{bot} and the top bubble V_{top} with error bars indicating the propagated systematic measurement error. The volume of bottom bubble never exceeds one third of the volume of the top one. The smallest bottom bubble compared to its top one is 10 times smaller than its predecessor. Figure 8 c) illustrates the ratio between the sum of the volumes of the two bubbles $V_{bot}+V_{top}$ immediately before coalescence and the total volume V_{coal} just after (1ms). After coalescence the total volume is 5-18% larger than before. This suggests that the process of coalescence causes a brief increase in heat transfer to the liquid-vapour interface. This might occur at the base of the second bubble, or by heat transfer from a thin superheated liquid layer trapped between the bubbles, or by rapid motion close to the line of coalescence.

CONCLUSIONS

Bubble growth from an isolated artificial cavity at the end of the isolated bubble regime and the beginning of the regime of interference, where vertical coalescence appears, has been experimentally investigated. The phenomenon of vertical coalescence was visualised and quantified using high-speed imaging. Further studies of longer sequences at different wall superheats and pressures of 0.5 bar, 0.75 bar and 1 bar revealed the dependence of vertical coalescence on these properties.

a)   b)   c)
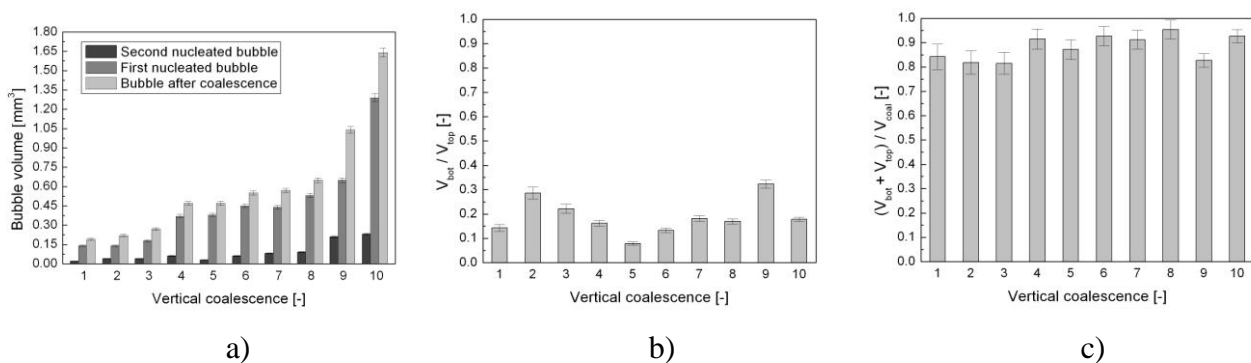
Figure 8. a) Bubble volume immediately before coalescence and the total volume after for 10 pairs of bubbles. b) Ratio between the volume of the newly nucleated bubble (bottom bubble) and the previously departed bubble (top bubble) for the same 10 bubble pairs. c) Ratio of the total volume of the top and bottom immediately before coalescence and the volume of the coalesced bubble.

With increasing wall superheat bubble growth changes from the isolated bubble regime into the regime of interference. The average frequency of bubble nucleation and vertical coalescence increased with the wall superheat. Decreasing the pressure, increases the average frequency of vertical coalescence and therefore subsequently the average frequency of nucleated bubbles from the artificial cavity. At 0.5 bar every two nucleated bubble pairs merge into one for high wall superheats. At 1 bar up to three single bubbles depart from the artificial cavity, before two coalesce.

The equivalent volume of a sphere was calculated for ten pairs of bubbles immediately before and after they coalesced. The second nucleating bubble is always smaller than its departed predecessor. During coalescence the vapour volume still increases, as the merged bubble is between 5 and 18% larger than the summarised volumes of the two bubbles before coalescence.

NOMENCLATURE

Nu	number of bubble nucleations	[-]
p	pressure	[Pa]
p_g	vapour pressure	[Pa]
p_l	liquid pressure	[Pa]
r_b	bubble radius	[m]
r_c	cavity mouth radius	[m]
T_{sat}	saturation temperature	[°C]
V	volume	[m^3]
V_{bot}	bottom bubble vapour volume	[m^3]
V_{coal}	upper bubble vapour volume	[m^3]
V_{top}	coalesced bubble vapour volume	[m^3]
VC	number of vertical coalescence	[-]
y	variable in vertical direction	[m]
σ	surface tension	[N/m]

ACKNOWLEDGEMENTS

REFERENCES

1. Zuber, N., Nucleate Boiling. The Region of Isolated Bubbles and the Similarity with Natural Convection, *Int. J. Heat Mass Transfer*, vol. 6, pp. 53-78, 1963.
2. Dhir, V.K., Boiling Heat Tranfer, *Annu. Rev. Fluid. Mech.*, 30, pp. 365-401, 1998.
3. Buyevich, Y.A. and Webbon, B.W., The Isolated Bubble Regime in Nucleate Boiling, *Int. J. Heat Mass Transfer*, vol.2, no.2, pp. 365-377, 1997.
4. Zhang, L. and Shoji, M., Nucleation Site Interaction in Pool Boiling on the Artificial Surface, *Int. J. Heat Mass Transfer*, 46, pp. 513-522, 2003.
5. Bankoff, S.G., Entrapment of Gas in the Spreading of a Liquid over a Rough Surface, *AIChE Journal*, vol. 4, no. 1, pp. 24-26, 1958.
6. Bonjour, J., Clausse, M. and Lallemand, M., Experimental Study of the Coalescence Phenomenon During Nucleate Pool Boiling, *Exp. Therm. Fluid Science*, 20, pp. 180-187, 2000.